

Communities at Work: The Making of Çatalhöyük

Edited by

Ian Hodder & Christina Tsoraki

Colour figures for Chapter 9. The complexity of open spaces at Çatalhöyük

*Justine Issavi, Lucy Bennison-Chapman, Amy Bogaard, Lindsay Der, Sean Doyle,
Aroa García Suárez, Scott D. Haddow, Ceren Kabukcu, Kamilla Pawłowska, Heeli Schechter,
Duygu Tarkan, Christina Tsoraki, Milena Vasić, Rena Veropoulidou & Jesse Wolfhagen*

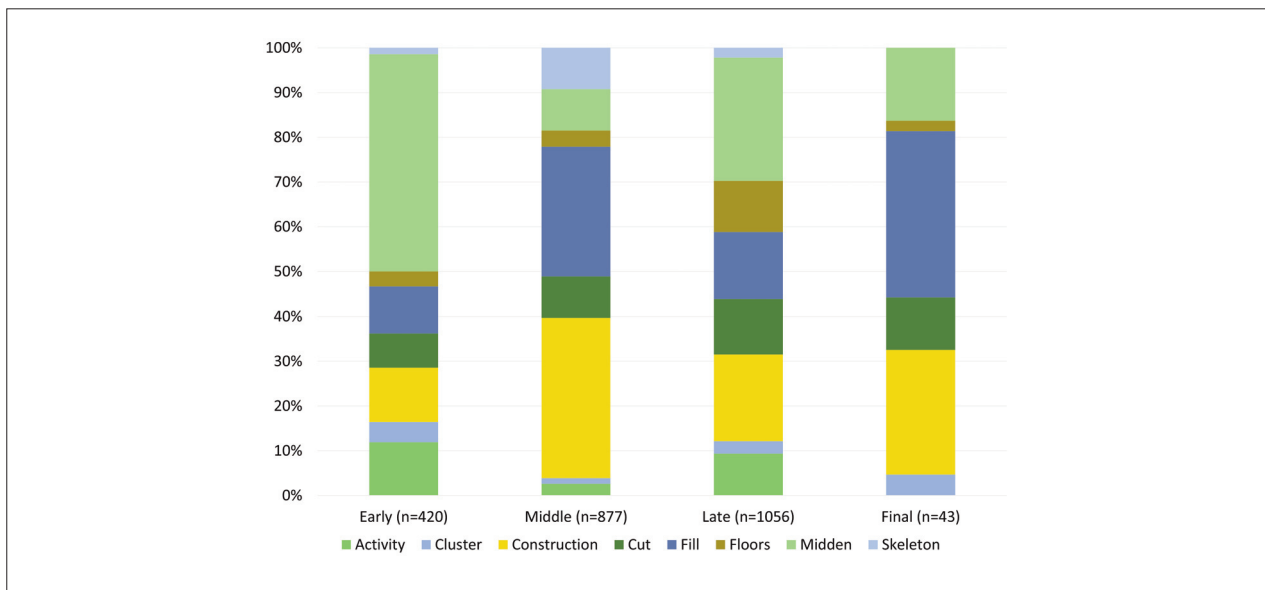


Figure 9.4. Percentage of external units by data category, through time.

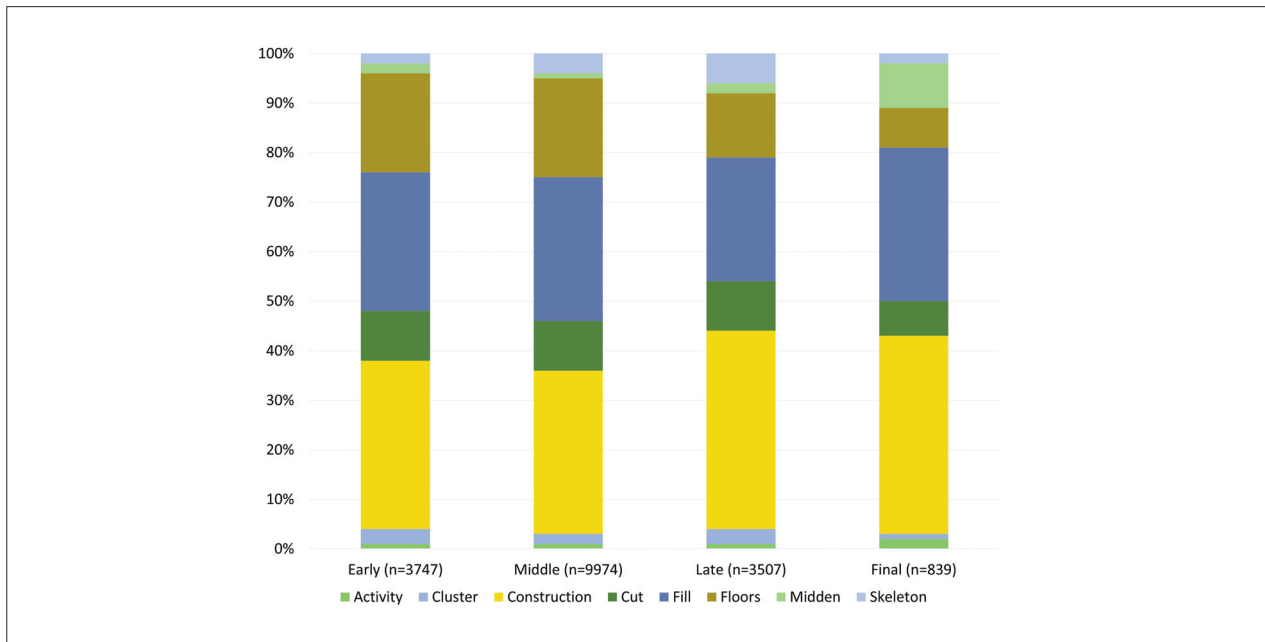


Figure 9.5. Percentage of internal units by data category, through time.

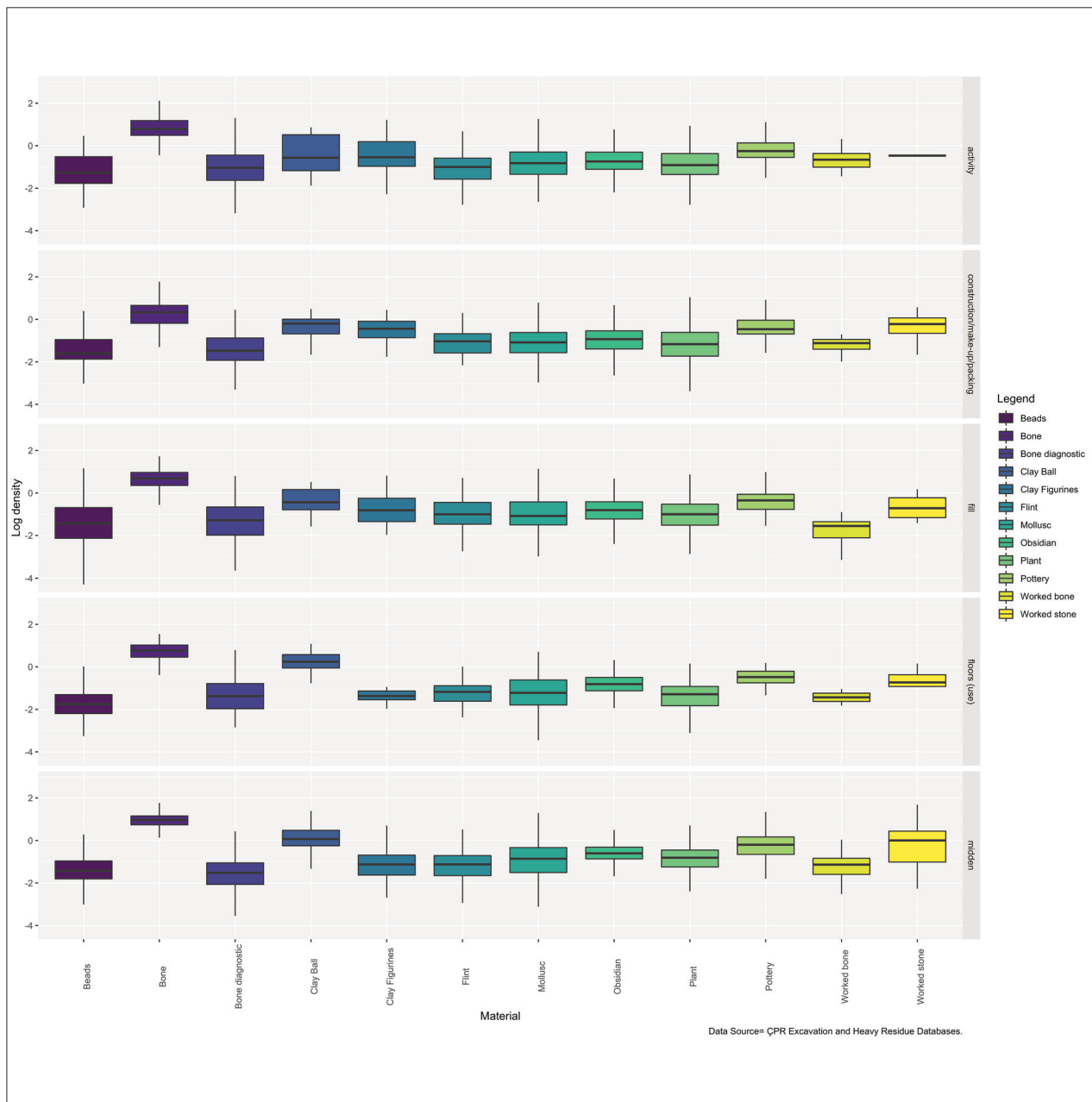


Figure 9.11. Overall logged density of finds in open spaces by data category.

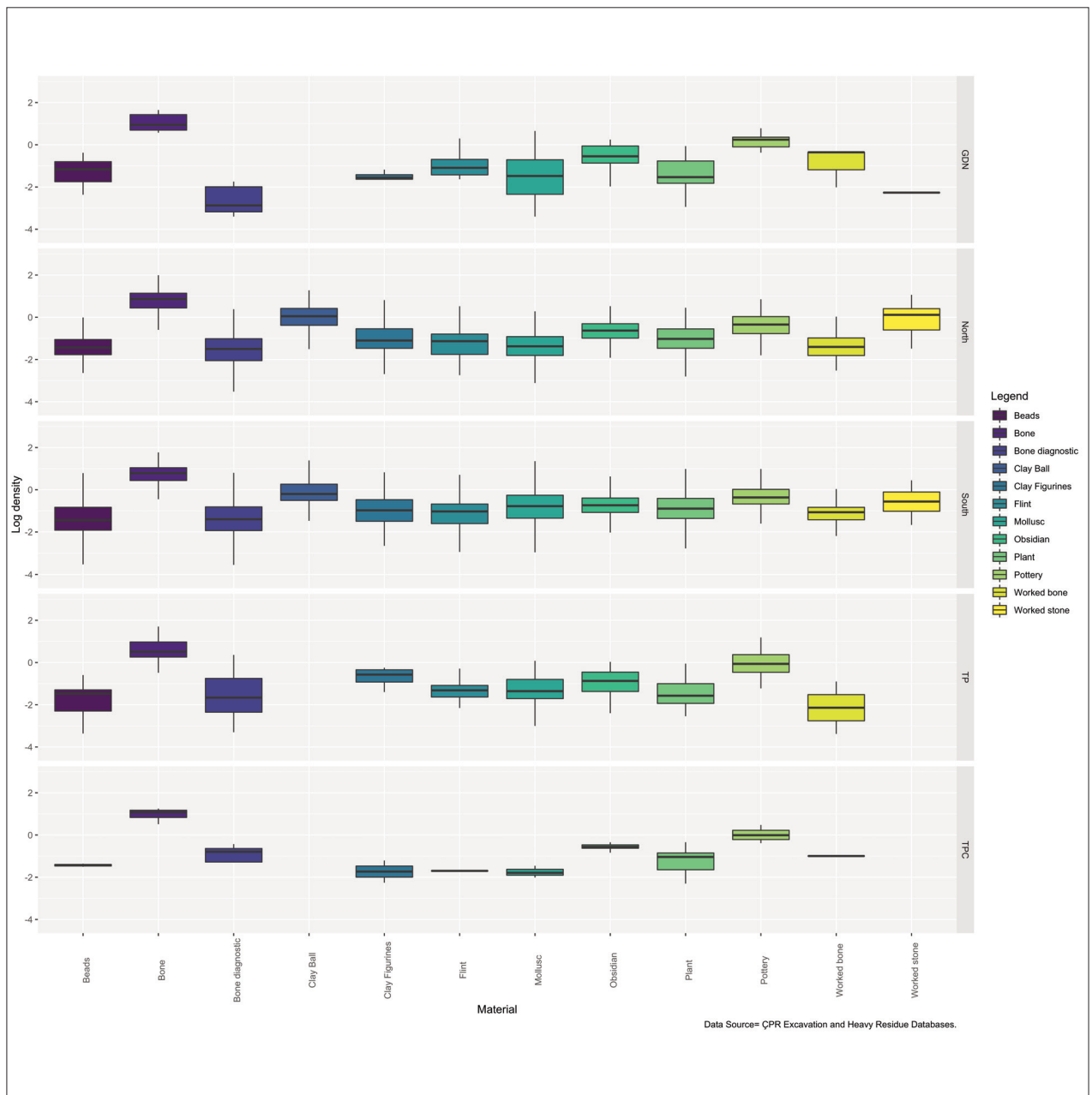


Figure 9.12. Overall logged density of finds in open spaces by Area.

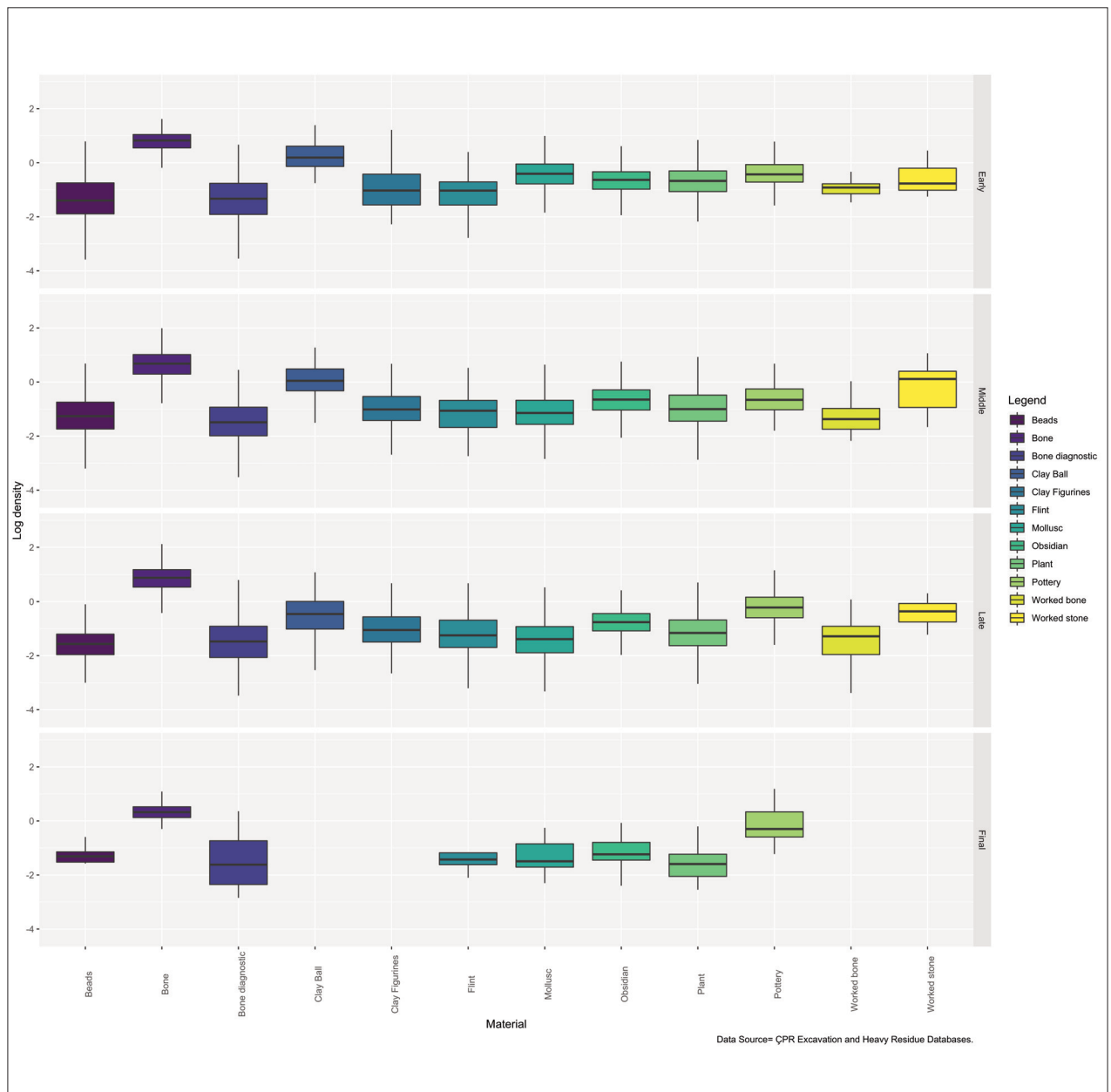


Figure 9.13. Overall logged density of finds in open spaces by occupation period.

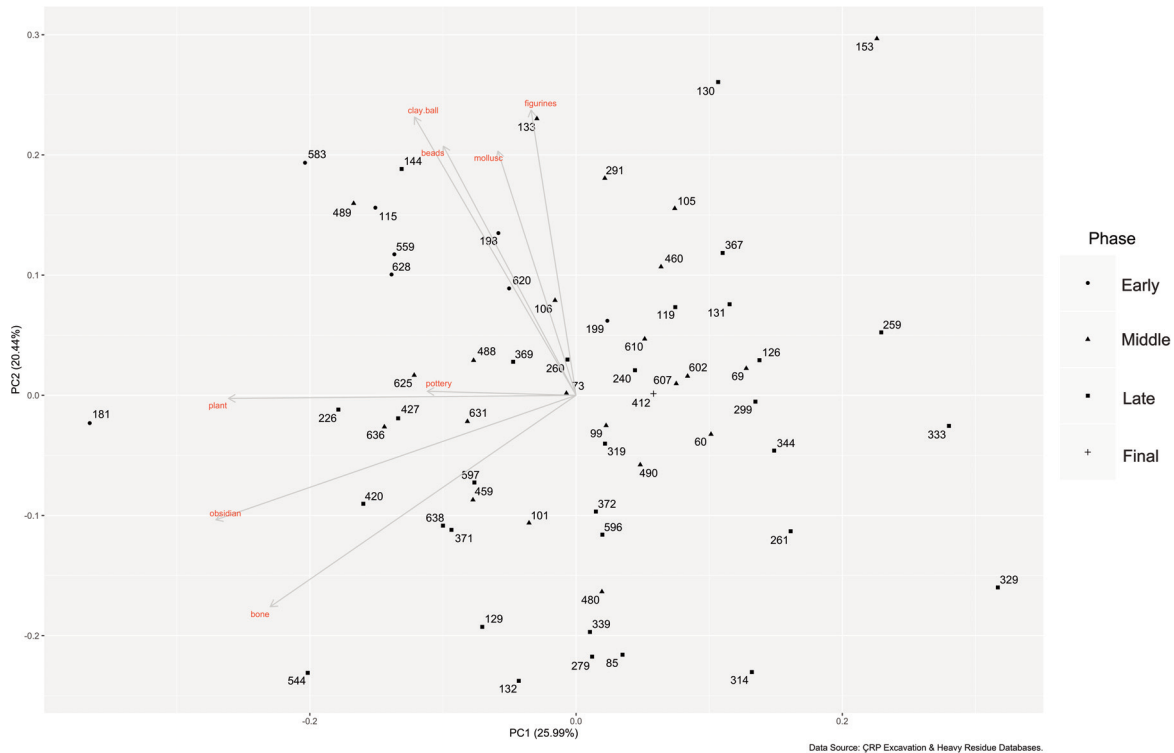


Figure 9.15. PCA biplot based on heavy residue densities (g/L). Spaces are grouped by time period.

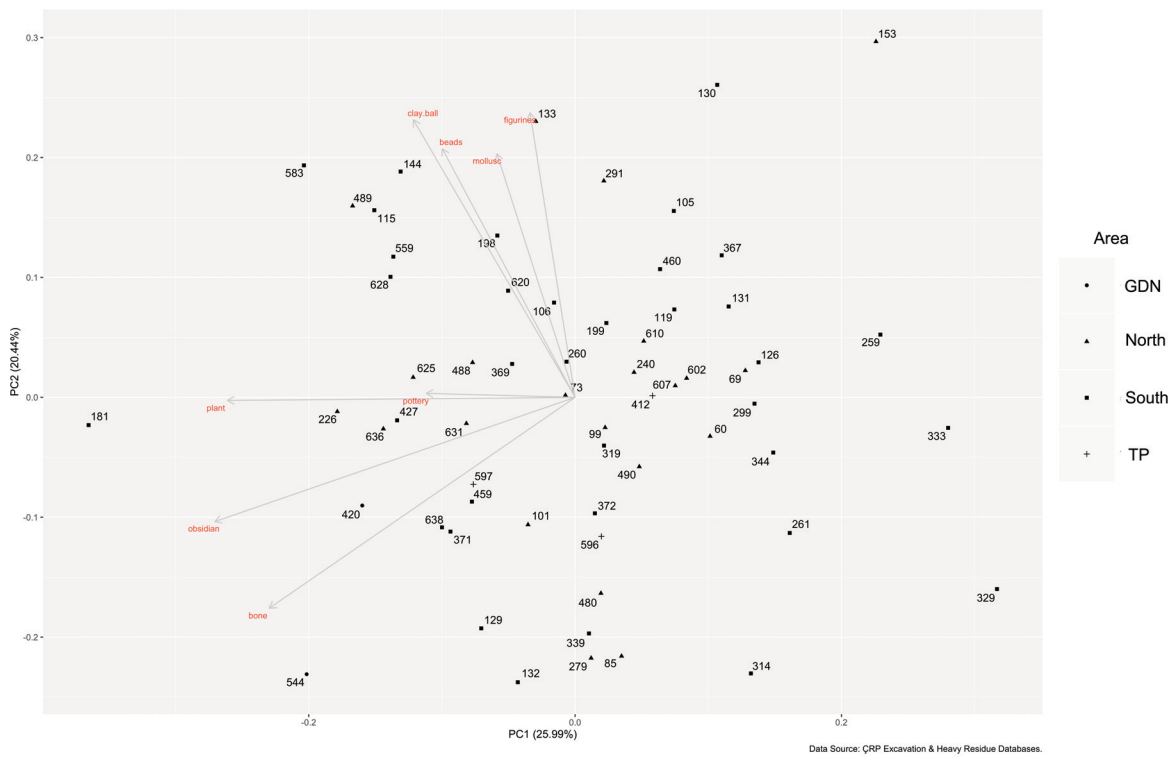


Figure 9.16. PCA biplot based on heavy residue densities (g/L). Spaces are grouped by area.

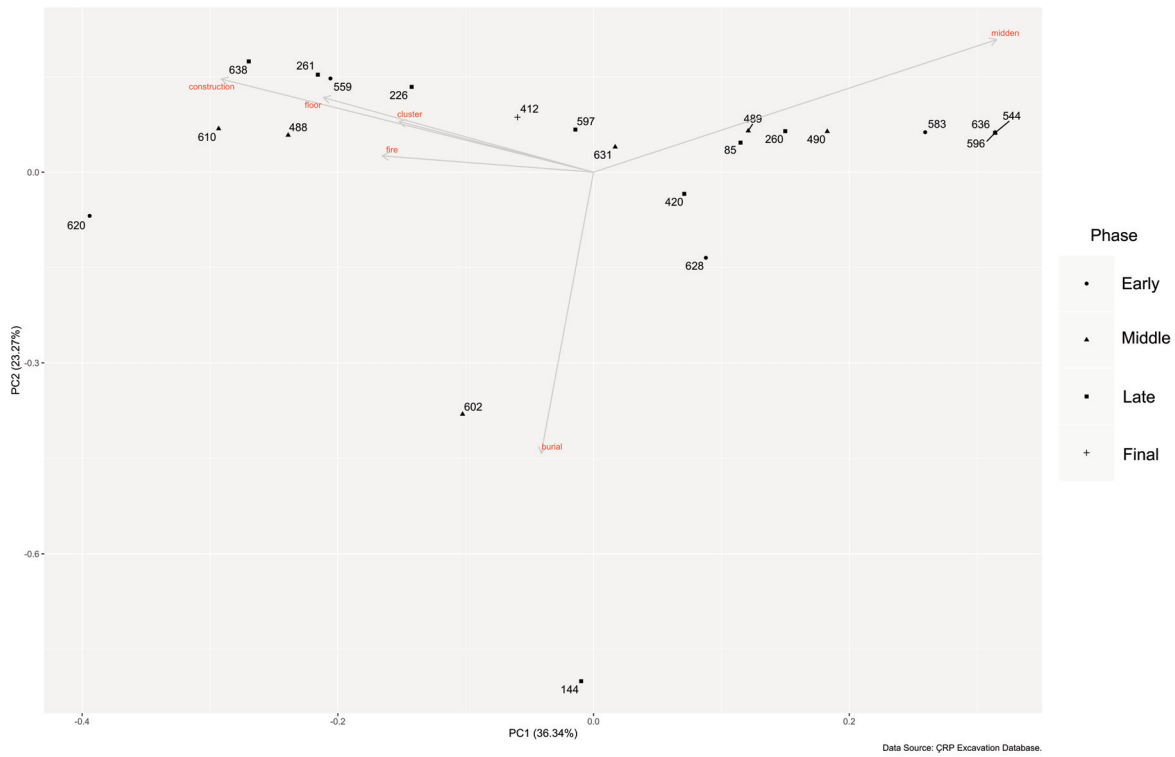


Figure 9.18. Biplot of unit-type composition PCA results grouped by occupation period.

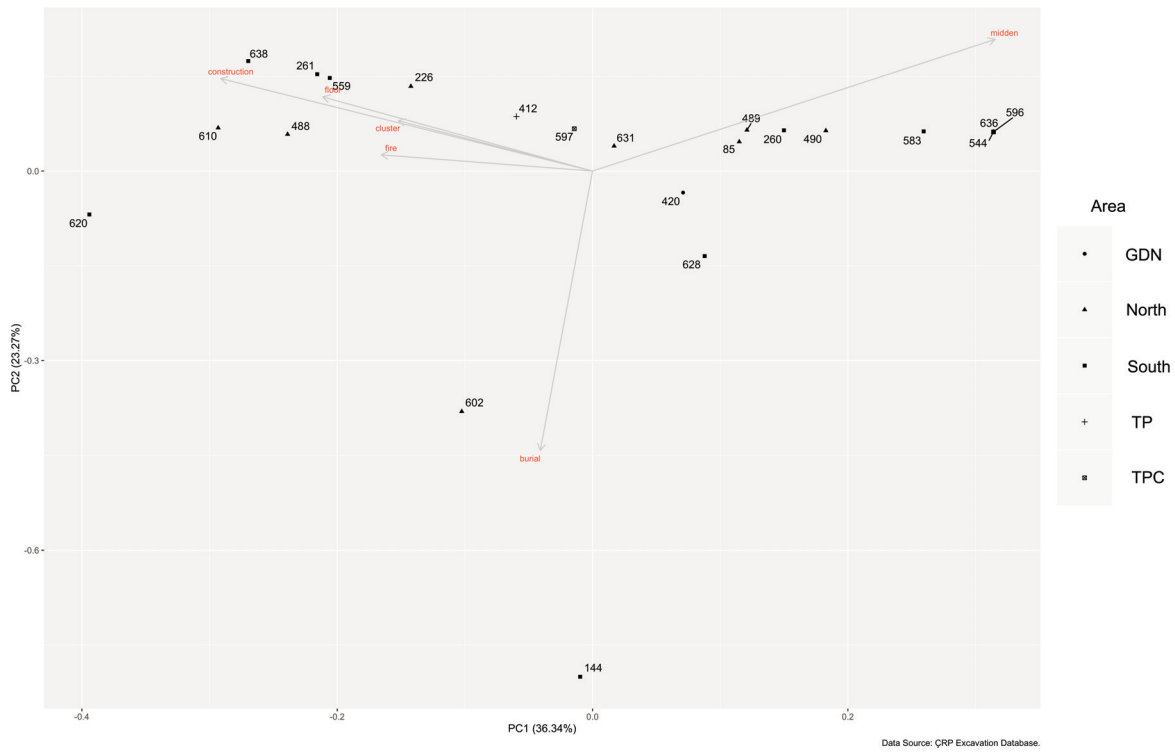


Figure 9.19. Biplot of unit-type composition PCA results grouped by excavation area.

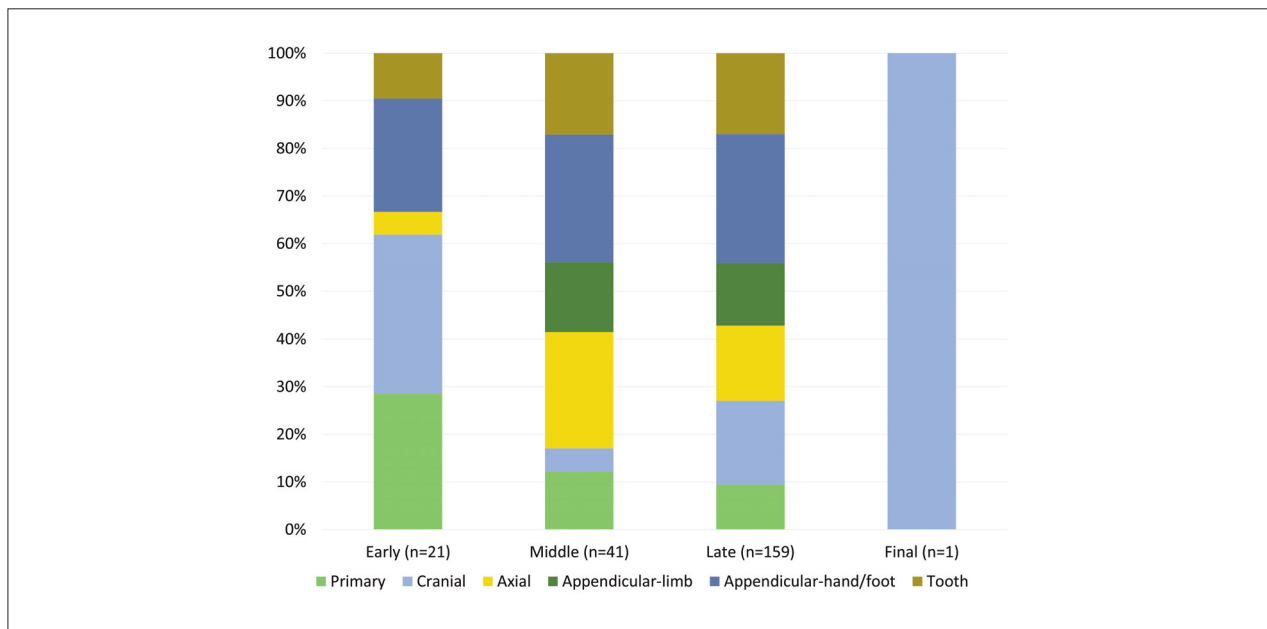


Figure 9.21. Tertiary human remains by element, through time.

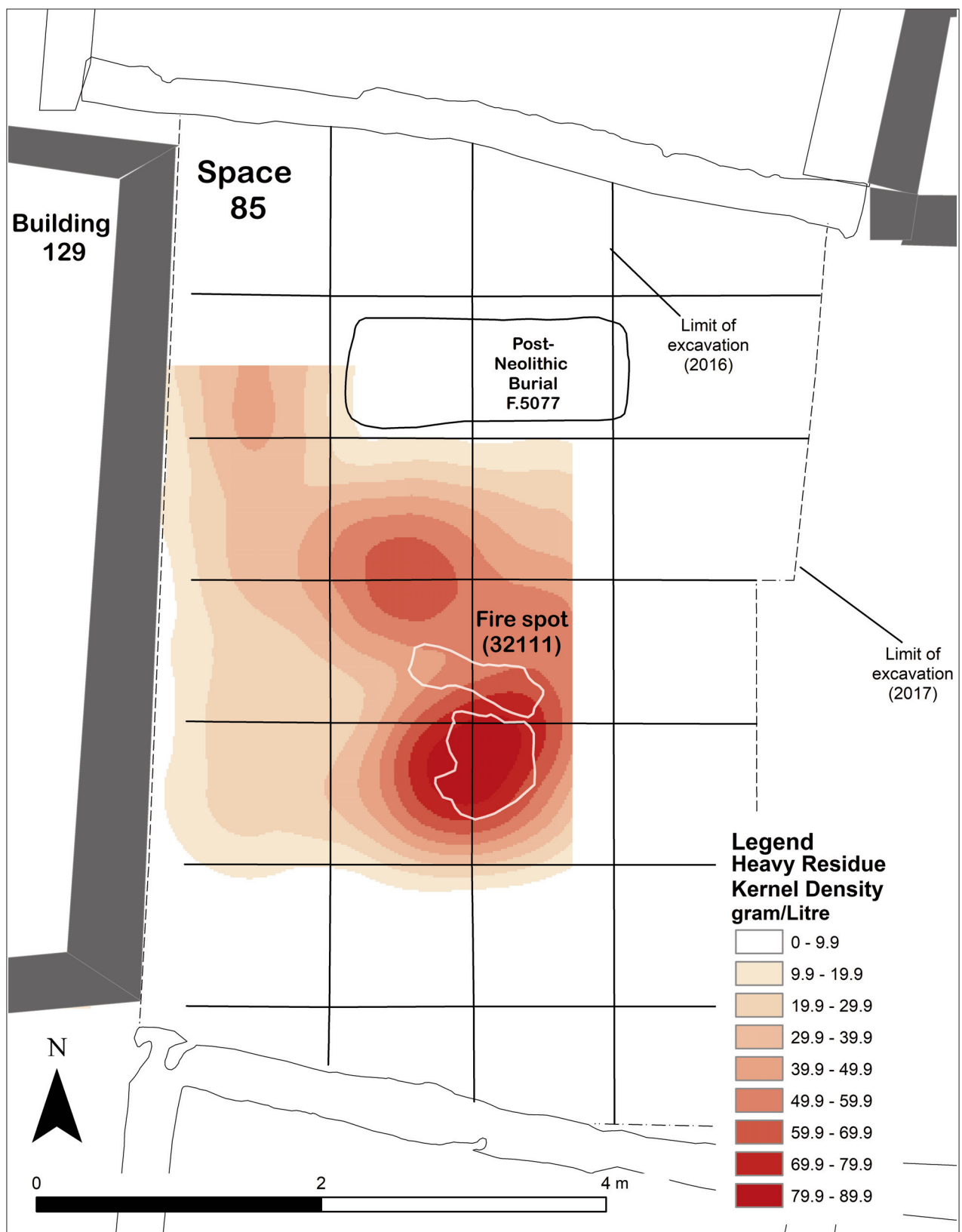


Figure 9.22a. Kernel densities for all finds classes through space and time: Sp.85.

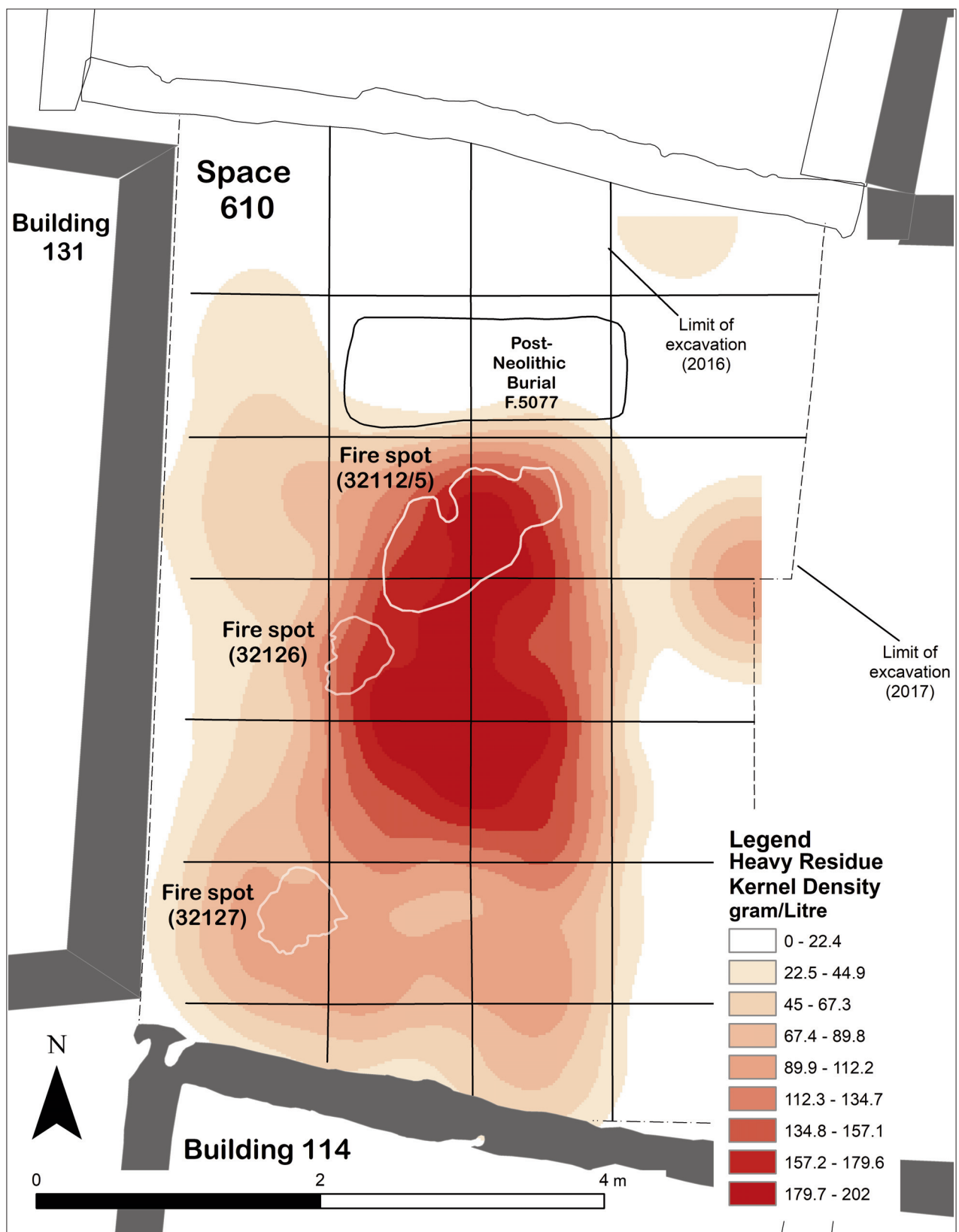


Figure 9.22b. Kernel densities for all finds classes through space and time: Sp.610.

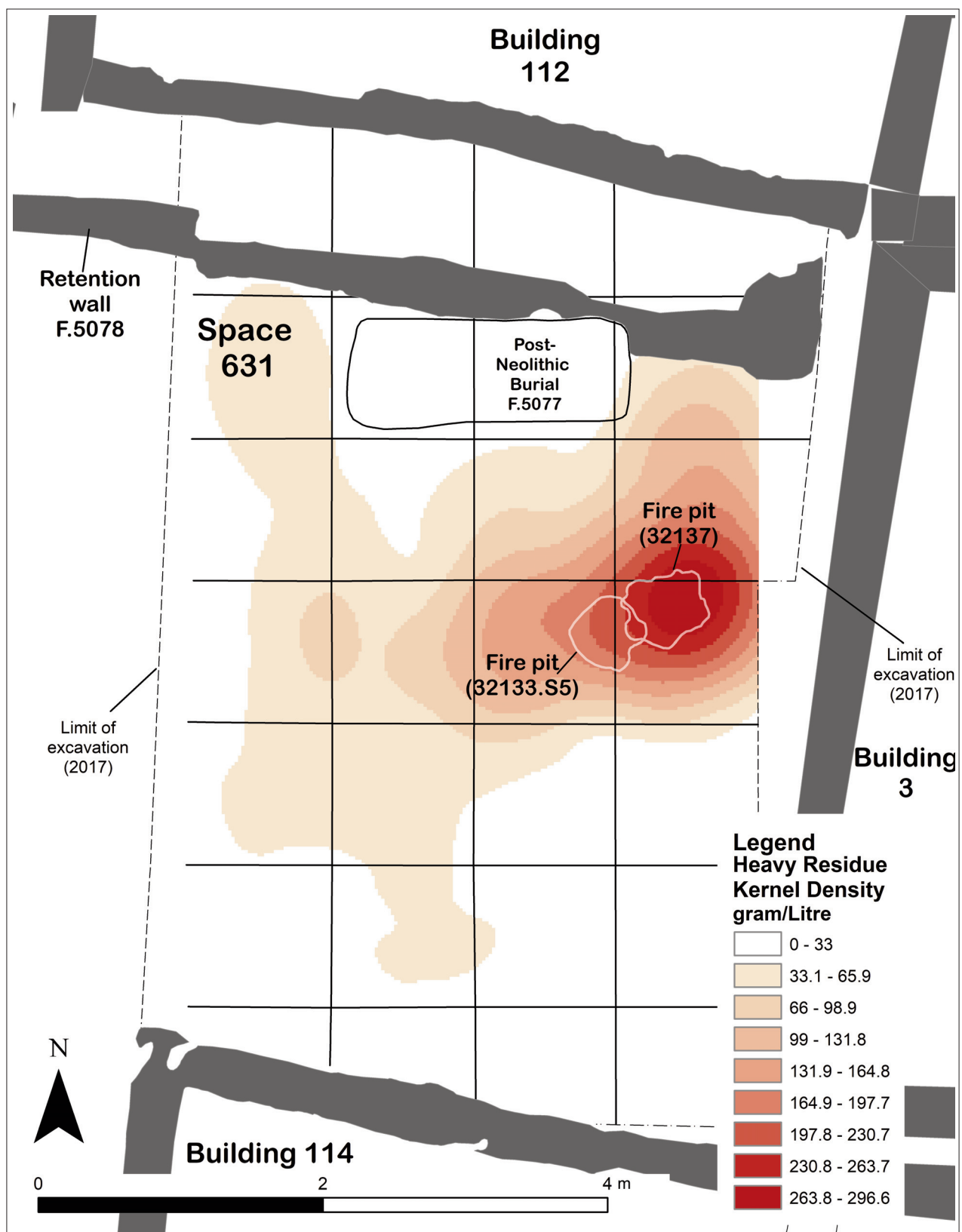


Figure 9.22c. Kernel densities for all finds classes through space and time: Sp.631.

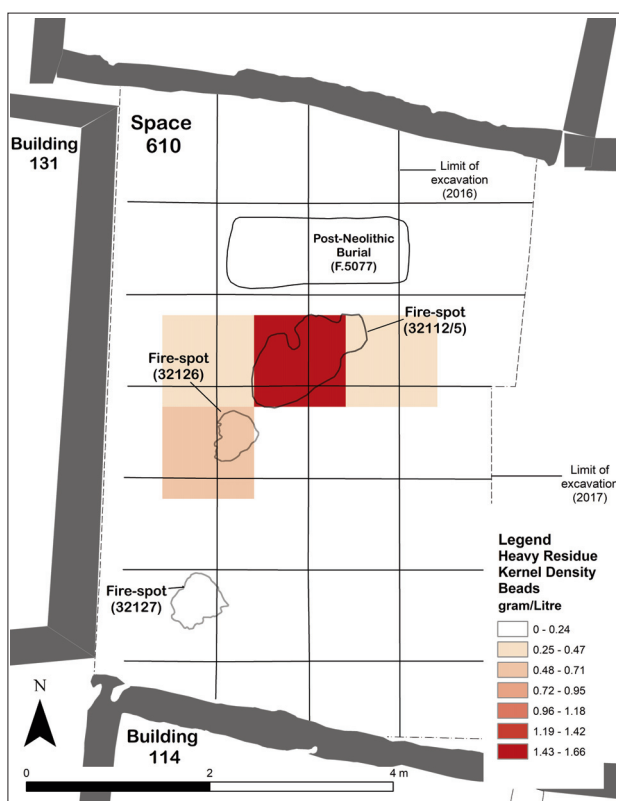
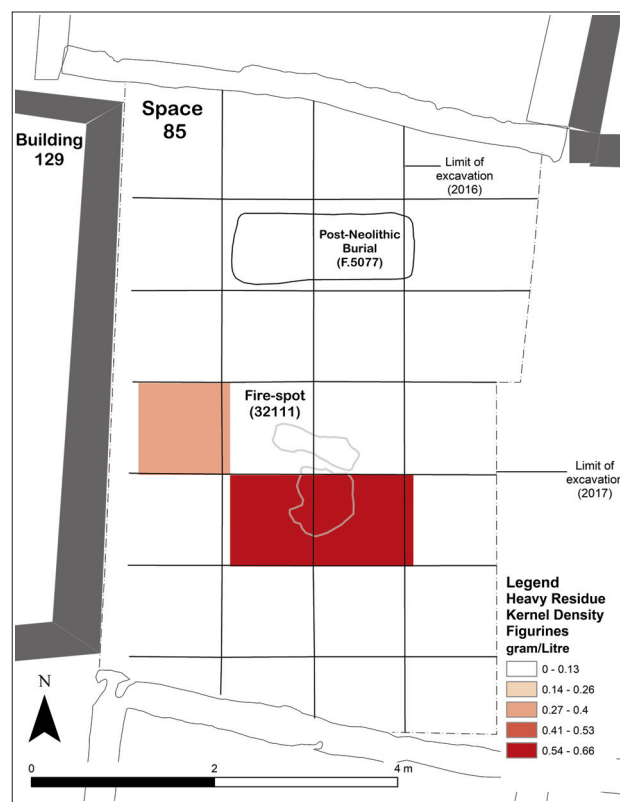
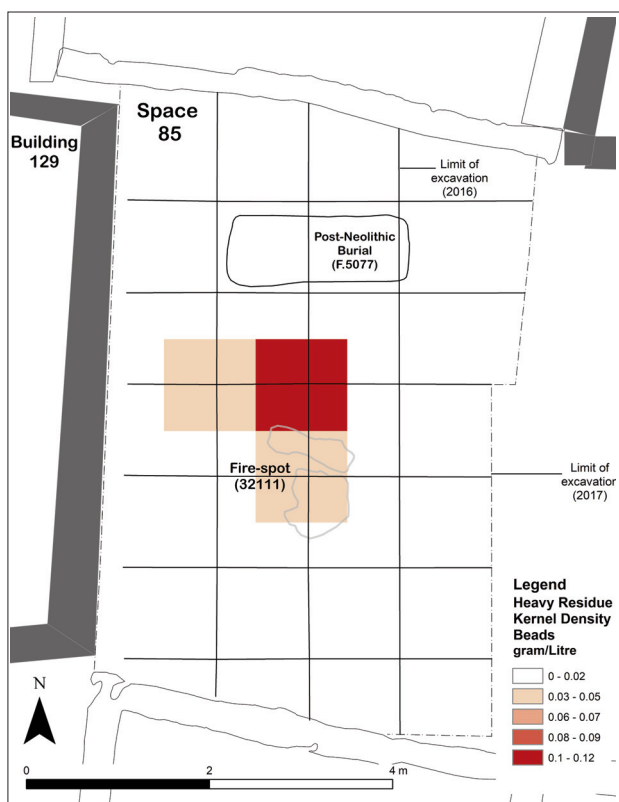


Figure 9.23. Spatial distribution of beads in Sp.85 and Sp.610.

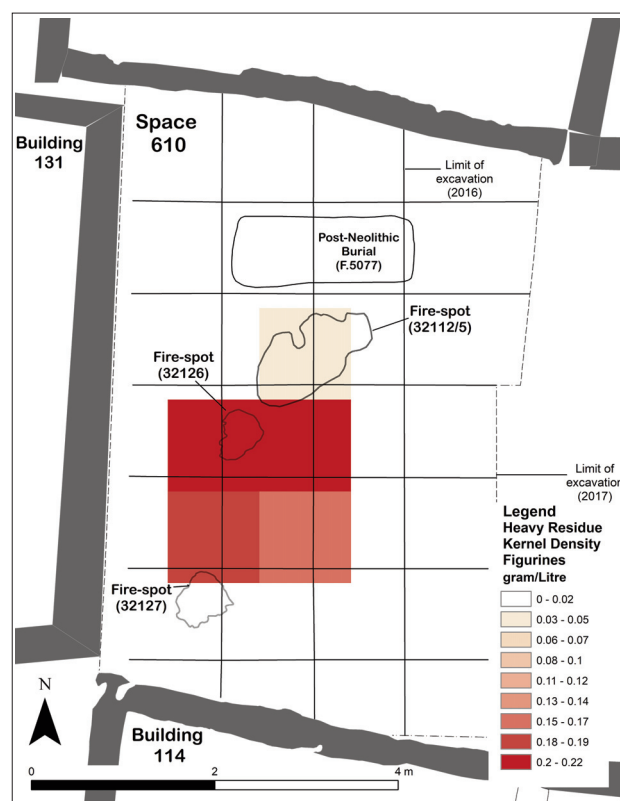


Figure 9.24. Spatial distribution of figurines in Sp.85 and Sp.610.

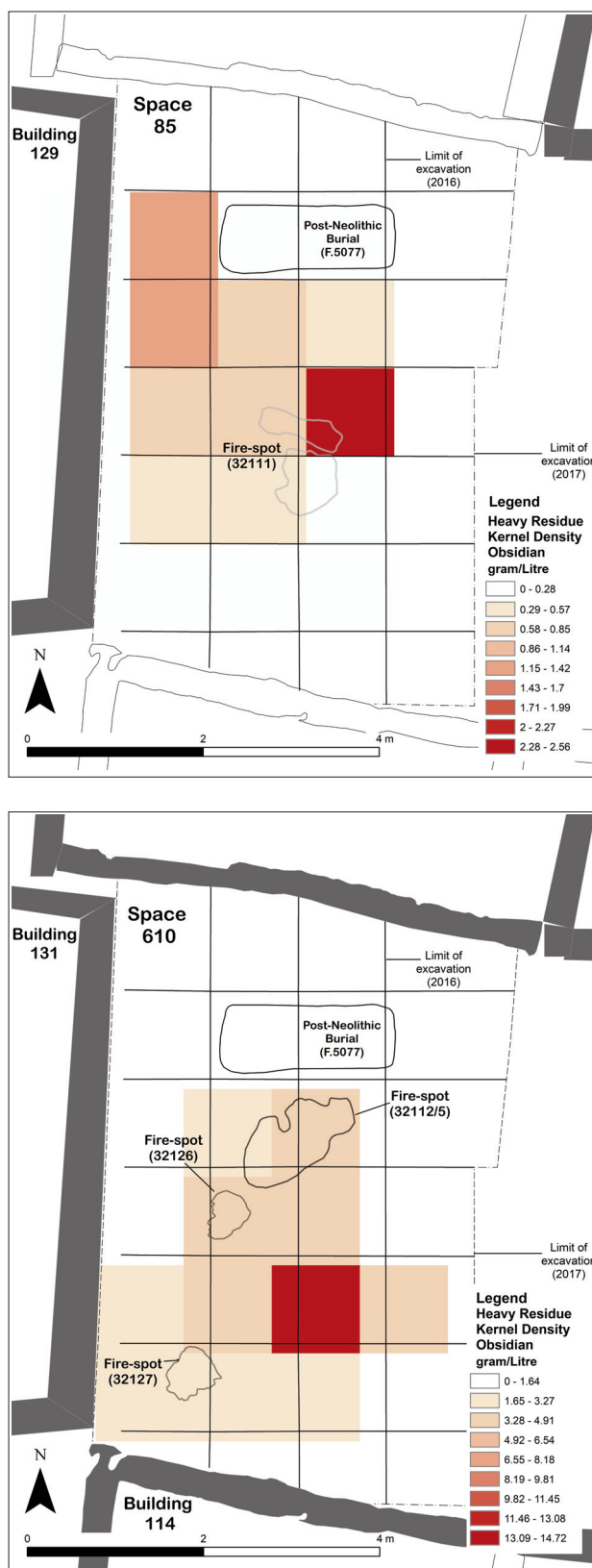


Figure 9.25. Spatial distribution of obsidian in Sp.85 and Sp.610.